

Ternary Polymer Composites: PA6,6/Maleated SEBS/Glass Beads

S. C. TJONG,¹ S. A. XU²

¹ Department of Physics and Materials Science, City University of Hong Kong, Tat Chee Avenue, Kowloon, Hong Kong, China

² Institute of Polymer Science and Engineering, East China University of Science and Technology, 130 Mei-Long Road, Shanghai, China

Received 18 May 2000; accepted 29 November 2000

ABSTRACT: Polyamide 6,6 (PA6,6)/maleated styrene–hydrogenated butadiene–styrene (SEBS) blends filled with up to 20% spherical glass beads (GBs) were prepared by extrusion and subsequent injection molding. Tensile and impact tests were used to examine the effect of GB additions on the mechanical behavior of PA6,6/SEBS-*g*-MA 80/20 blend. Tensile measurements showed that the GB additions improve the stiffness of the PA6,6/SEBS-*g*-MA 80/20 blend but had little effect on its tensile ductility. The impact test revealed that the impact strength of PA6,6/SEBS-*g*-MA 80/20 blend tends to decrease with increasing GB content. Therefore, the GB additions were beneficial to maintain a stiffness-to-toughness balance of the PA6,6/SEBS-*g*-MA 80/20 blend. Finally, the correlation between the experimental tensile stiffness and strength with various theoretical models is discussed. © 2001 John Wiley & Sons, Inc. *J Appl Polym Sci* 81: 3231–3237, 2001

Key words: polyamide 6,6; styrene–hydrogenated butadiene–styrene; glass bead; stiffness; strength; compatibility

INTRODUCTION

There has been considerable interest to modify the properties of raw polymers from both a practical and a scientific point of view. This can be achieved by polymer blending and composite compounding. Polymer blends generally inherit good properties from their parent polymers. The combination of two or more commercially available polymers through blending represents an effective and low-cost technique for tailoring of new materials. The composite compounding involves

the addition of mineral fillers, whiskers, or fibers into the polymer matrix. In general, mineral fillers impart high stiffness but low tensile strength to polymers because of their low aspect ratio values. In contrast, whisker or fiber additions can lead to a dramatic improvement in the mechanical stiffness, hardness, and strength of polymers.^{1–3}

Aliphatic polyamides (PA) such as PA6,6 and PA6 are widely used as structural materials in automotive industries because of their high melting temperatures, high strength, and good chemical resistance. However, polyamides suffer from high moisture absorption and high impact notch sensitivity. The impact toughness of PA can be improved by the addition of elastomers. The cavitation of elastomer particles and associated ma-

Correspondence to: S. Tjong.
Contract grant sponsor: Croucher Foundation of Hong Kong.

Journal of Applied Polymer Science, Vol. 81, 3231–3237 (2001)
© 2001 John Wiley & Sons, Inc.

trix shear yielding are the main toughening mechanisms for PA/elastomer blends. This toughness improvement is achieved at the expense of stiffness and strength characteristics. Polyamides have been successfully toughened by various elastomers such as ethylene-propylene-diene monomer rubber (EPDM), ethylene-propylene rubber (EPR), and styrene-hydrogenated butadiene-styrene triblock copolymers (SEBS).⁴⁻⁹

Blends of polyamides and unfunctionalized rubbers tend to have low impact toughness because the elastomeric particles formed during melt blending are relatively large. The compatibility between PA and elastomers can be enhanced by the addition of a compatibilizer. In this respect, elastomers are grafted with functional groups such as maleic anhydride (MA) prior to blending with PA. These functional groups react with the amine end groups of PA, leading to both a finer dispersion of elastomers and a better adhesion between the elastomers and PA matrix. Consequently, the elastomers act as stress concentrators favoring the dissipation of impact energy. Oshinski et al.⁷ reported that PA6 can be toughened by blending with appropriate combinations of SEBS and SEBS-*g*-MA. This is because pure SEBS particles are too large for toughening PA6, whereas SEBS-*g*-MA particles are too small for optimal toughening. On the other hand, PA6,6 can be toughened by blending with SEBS-*g*-MA alone, and addition of SEBS merely reduced toughness.⁸ In other words, melt-blending of SEBS-*g*-MA with PA6,6 results in particles with optimal size for toughening. These results may be attributed to differences observed in the morphology of the two blends. They further suggested that PA6 is monofunctional, whereas PA6,6 is difunctional in its reactions with anhydride.⁸

In general, the tensile strength and stiffness of the PA tend to decrease with increasing elastomer content.^{6,8} It is appropriate to add fillers into elastomer-toughened PA to improve the stiffness-to-toughness balance. The structure and mechanical properties of three-component or ternary hybrid composites are very complex; they depend on the component properties such as compatibility, the characteristics of each component, volume fractions of fillers and elastomers, and processing conditions. The microstructures of ternary composites vary from the case where elastomers and fillers are dispersed separately in the matrix to a core-shell morphology, in which the elastomer particles with filler core are distributed in the

Table I Size Distribution of Glass Beads

| | Diameter (μm) | | | |
|------------|----------------------------|-----|-----|------|
| | 10% | 50% | 90% | Mean |
| Glass bead | 13 | 32 | 61 | 35 |

matrix. Efforts have been made by some workers to incorporate inorganic fillers⁹⁻¹² and glass beads (GBs)¹³⁻¹⁵ into elastomer-toughened polypropylene. For example, Jancar and Dibenedetto¹⁰ reported that the inorganic filler [CaCO_3 or $\text{Mg}(\text{OH})_2$] is encapsulated by ethylene-propylene elastomer (EPR) when adhesion between the elastomer phase and rigid filler is enhanced by addition of a compatibilizer. The formation of core-shell inclusions changes the main failure mechanism from unstable localized shear bonding, nucleated at the filler surface, to delocalized shear yielding.

In this study, we attempt to add GBs into PA6,6/SEBS-*g*-MA blend. GBs are selected because of their regular spherical shape, thereby yielding isotropic mechanical properties. Moreover, polymers filled with GBs have good processability and high dimensional stability.¹⁶ Although PA/elastomer blends have been studied extensively, relatively less information is available on the effect of fillers on the mechanical properties of these blends. This investigation aims to study the effect of glass bead additions on the mechanical properties of PA6,6/SEBS-*g*-MA blend. Particular attention is paid to the tensile characteristics.

EXPERIMENTAL

Materials

PA6,6 used in this study was supplied by Mitsubishi Engineering Plastics Company (Taiwan). Spherical glass beads with the trade name of Spheriglass were purchased from Potters Industry Inc., and the density was 2.5 g/cm^3 . The glass beads received no surface treatment. The size distribution of GBs is listed in Table I. Maleic anhydride-grafted SEBS, designated as SEBS-*g*-MA, was kindly supplied by the Shell Company under the trade name Kraton G 1901X. The triblock copolymer with styrene end blocks and a hydrogenated butadiene midblock was grafted with 1.84 wt % MA.

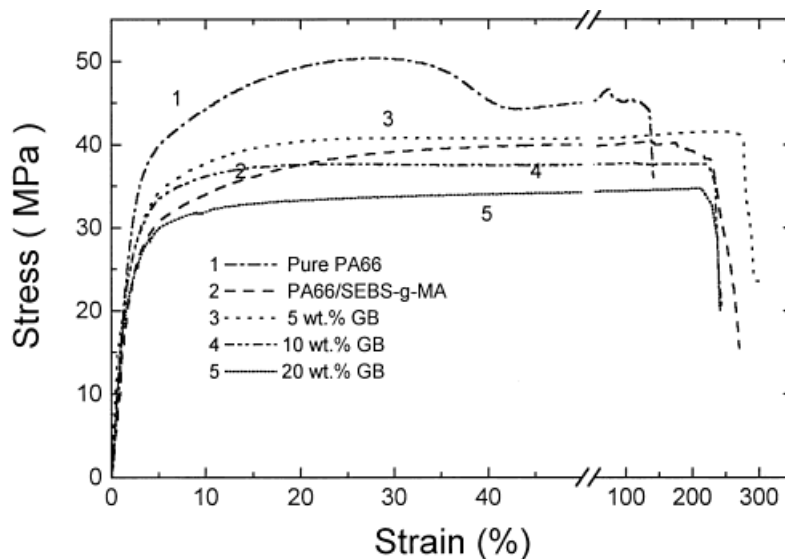


Figure 1 Typical stress-strain curves of pure PA6,6, PA6,6/SEBS-*g*-MA blend, and its composites.

Sample Preparation

All materials used were dried in ovens for 48 h, at 80°C for PA6,6 and GBs and at 60°C for SEBS-*g*-MA. The composition of the matrix of composites was fixed at 80 wt % PA6,6 and 20 wt % SEBS-*g*-MA. The PA6,6/SEBS-*g*-MA 80/20 blend and hybrid composites containing 5, 10, 15, and 20 wt % GBs were prepared in a twin-screw Brabender Plasticorder at 270°C. The extrudates were cut into pellets by a pelletizer. Using these pellets, the plaques (200 × 80 × 3.2 mm) were injection molded. The barrel zone temperatures were set at 270, 270, and 240°C.

Mechanical Properties

Dumbbell-shaped tensile bars (according to ASTM 638) were cut from the plaques. The tensile behavior of specimens was determined using an Instron tensile tester (model 4206) under a cross-head speed of 10 mm/min at 23°C. At least five specimens of each composition were tested and the average values reported. The fracture surfaces of specimens after tensile tests were examined in a JEOL scanning electron microscope (model JSM 820; JEOL, Peabody, MA).

Notched Izod impact specimens (65 × 12.7 × 3.2 mm) were prepared from the injection-molded plaques. Seven specimens were tested and the average values reported.

RESULTS AND DISCUSSION

Mechanical Properties

Figure 1 shows the typical stress-strain curves for pure PA6,6, PA6,6/SEBS-*g*-MA 80/20 blend, and hybrid composites containing various contents of GBs. Apparently, PA6,6 exhibits a typical behavior of engineering plastics with high tensile strength and stiffness. The addition of 20 wt % SEBS-*g*-MA leads to a decrease in both tensile strength and Young's modulus, particularly the stiffness. However, the elongation at break of the PA6,6/SEBS-*g*-MA 80/20 blend is more than twice that of pure PA6,6, indicating that super-tough nylon can be achieved by blending PA6,6 with SEBS-*g*-MA impact modifier. This result is expected, given that maleated SEBS exhibits a low stiffness.

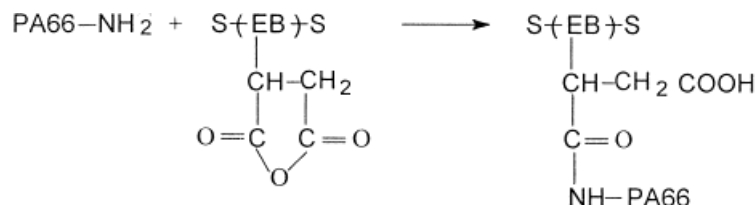
Table II summarizes the average values for tensile and impact parameters of all specimens tested. This table reveals that the stiffness of PA6,6/SEBS-*g*-MA 80/20 blend tends to increase with increasing GB content. The addition of GBs up to 20 wt % to the PA6,6/SEBS-*g*-MA 80/20 blend leads to only a small decrease in yield strength and elongation at break. Moreover, impact measurements indicate that pure PA6,6 exhibits the lowest impact energy of 2.6 kJ/m². The addition of SEBS-*g*-MA copolymer to PA6,6 results in a dramatic increase in its impact strength. Such an improvement in tensile ductil-

Table II Mechanical Properties of Specimens Investigated

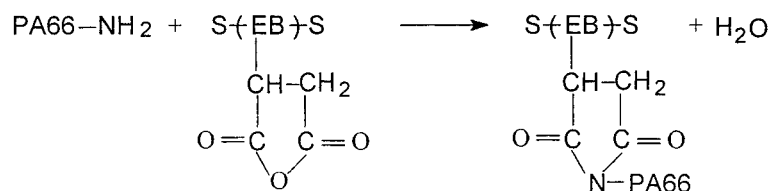
| Specimen | Stiffness (MPa) | Yield Strength (MPa) | Elongation at Break (%) | Fracture Energy (kJ/m ²) | Impact Strength (kJ/m ²) |
|--------------------------|-----------------|----------------------|-------------------------|--------------------------------------|--------------------------------------|
| PA6,6 | 1805 | 50 | 134 | 733 | 2.6 |
| PA6,6/SEBS- <i>g</i> -MA | 825 | 40 | 289 | 1208 | 67.7 |
| Composite-5 wt % GB | 976 | 41 | 316 | 1322 | 34.9 |
| Composite-10 wt % GB | 1147 | 38 | 276 | 1115 | 25.8 |
| Composite-15 wt % GB | 1061 | 39 | 291 | 1108 | 17.7 |
| Composite-20 wt % GB | 1133 | 34 | 274 | 1063 | 16.9 |

ity and impact toughness of PA6,6 is derived from the MA group of SEBS, which can react with the amine end groups of PA6,6 or possibly with the amide group to form imide linkages.¹⁷ SEBS is a hydrogenated form of a styrene/butadiene/styrene (SBS) block copolymer. MA can be grafted to

the EB chain to improve the properties of polymers, by providing polarity to enhance the adhesion and compatibility with other polymers and fillers. The reaction that takes place between PA6,6 and SEBS-*g*-MA copolymer during blending is shown as follows:



or



From Table II, the elongation at break of ternary composites is very close to that of PA6,6/SEBS-*g*-MA 80/20 blend. This implies that the addition of GBs has little effect on the tensile ductility of PA6,6/SEBS-*g*-MA 80/20 blend. The composite containing 5 wt % GB has a slightly higher elongation at break and fracture energy than those of PA6,6/SEBS-*g*-MA 80/20 blend. The increase in tensile ductility for this composite is possibly derived from the rigid glass bead particles, which act as obstacles to pin the propagating crack, thereby resulting the crack front to divert between the particles.¹⁸ However, the impact strength of PA6,6/SEBS-*g*-MA 80/20 blend tends to decrease with increasing GB content. The impact strength of composite containing 20

wt % GB is about fourfold higher than that of PA6,6. From the tensile and impact test results, it is evident that the addition of GBs exerts a beneficial effect to maintain a stiffness-to-toughness balance of the PA6,6/SEBS-*g*-MA 80/20 blend. The variation of Young's modulus of PA6,6/SEBS-*g*-MA 80/20 blend with GB content is shown in Figure 2. It is worth mentioning that GBs received no surface treatment with either silane coupling agent or MA. However, it is likely that the MA end group of PA6,6/SEBS-*g*-MA 80/20 blend can improve the interfacial adhesion between the matrix and GBs; in other words, there is some adhesion between the GBs and matrix. Such an improvement is beneficial to enhance the stiffness and yield strength of compos-

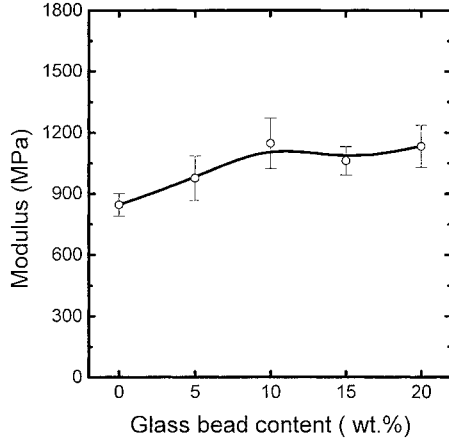


Figure 2 Variation of stiffness of PA6,6/SEBS-*g*-MA blend with GB content.

ites. From these results, it appears that pretreating the GBs with silane agent can further enhance the interfacial adhesion, although further work is needed to investigate this problem.

According to the literature, several empirical relationships have been proposed to predict the variation of stiffness with filler volume content for polymer composites. The simplest theoretical equation is Einstein's equation,¹⁹ which is valid only at low concentrations of filler and which assumes perfect adhesion between the filler and the polymer matrix, as well as perfect dispersion of filler particles. The equation reads

$$E_c = E_m(1 + 2.5\phi_f) \quad (1)$$

where E_c and E_m are the elastic modulus of the composite and the polymer matrix, respectively, and ϕ_f is the volume fraction of the filler. Guth²⁰ modified Einstein's equation into the following expression:

$$E_c = E_m(1 + 2.5\phi_f + 14.1\phi_f^2) \quad (2)$$

The empirical equation derived by Ishai and Cohen²¹ is

$$E_c = E_m \left[1 + \frac{\phi_f}{m/(m-1) - \phi_f^{1/3}} \right] \quad (3)$$

where $m = E_f/E_m$, and E_f is the elastic modulus of the fillers.

The most commonly used relationship is the Halpin-Tsai equation,²² which is given by

$$E_c = E_m \left(\frac{1 + \xi\eta\phi_f}{1 - \eta\phi_f} \right) \quad (4)$$

and

$$\eta = (m - 1)/(m + \xi) \quad (5)$$

where ξ is a measure of reinforcement and depends on the filler geometry, packing geometry, and loading directions. For spherical particles, $\xi = 2$.

The correlation between the theoretical prediction of the stiffness for filled polymers and the experimental data is shown in Figure 3. In this figure, the GB concentration is expressed in terms of volume content rather than the weight percentage. It can be seen that the experimental data are somewhat closer to empirical eqs. (1) and (3).

In general, most theoretical models provide better satisfactory bounds for modulus. The agreement between the theoretical prediction for yield strength and experiment is often not very good. This is because the yield strength models do not include the interfacial adhesion parameter. Interfacial filler-matrix adhesion plays an important role in the tensile yield behavior of filled polymer composites but it is a parameter that is difficult to measure. In the case of no interfacial adhesion, there is little stress transfer between the polymer and spherical fillers. The load is carried by the polymer matrix during tensile tests.

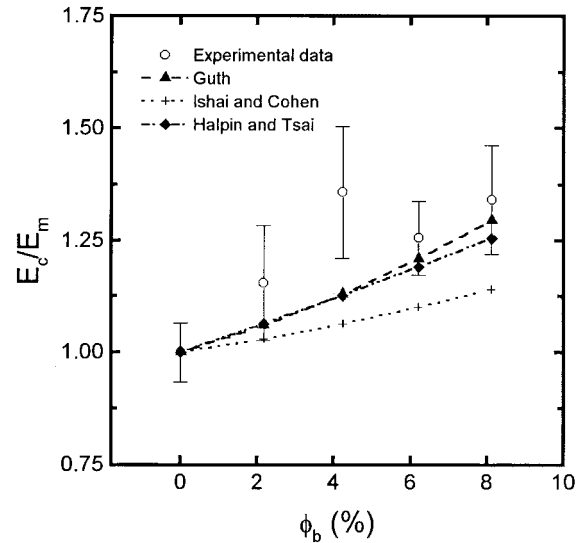


Figure 3 Experimental and theoretical plots showing the dependence of stiffness of PA6,6/SEBS-*g*-MA blend on glass bead volume content.

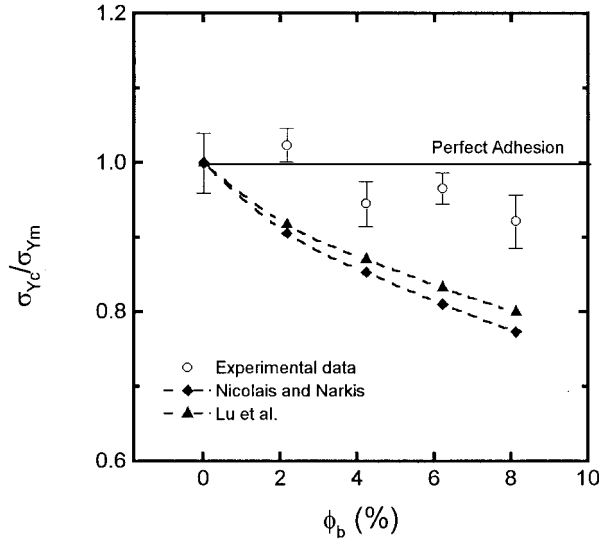


Figure 4 Experimental and theoretical plots showing the dependence of yield strength of PA6,6/SEBS-*g*-MA blend on glass bead volume content.

Nicolais and Narkis²³ derived the simple expression for spherical shape fillers in the absence of interfacial adhesion:

$$\sigma_{yc} = \sigma_{ym}(1 - 1.21\phi_f^{2/3}) \quad (6)$$

where σ_{yc} and σ_{ym} are the yield strength of the composite and matrix, respectively. When there is some adhesion between the filler and matrix, eq. (6) can be modified as

$$\sigma_{yc} = \sigma_{ym}(1 - 1.21 \sin^2\theta\phi_f^{2/3}) \quad (7)$$

where θ is the half debonding angle. Lu et al.²⁴ reported that θ is about 70° for spherical particles. Accordingly, eq. (6) can be rewritten as

$$\sigma_{yc} = \sigma_{ym}(1 - 1.07\phi_f^{2/3}) \quad (8)$$

The theoretical and experimental plots showing the relative yield strength versus GB volume content are shown in Figure 4. The horizontal line in this figure represents the upper bound relative strength for perfect adhesion. The curve based on the Nicolais–Narkis equation represents the lower bound strength ratio in the absence of interfacial adhesion. It can be seen from Figure 4 that the experimental data obtained for ternary composites could not be fitted with the above-described models. The experimental data values show positive deviation from the theoretical curve

predicted by Nicolais and Narkis, indicating there is some adhesion between the GBs and the matrix.

Morphology

Figure 5 is a SEM micrograph showing the fracture surface of PA6,6/SEBS-*g*-MA 80/20 blend after a tensile test. Extensive fibrillation of matrix can be seen in this micrograph, indicating that shear deformation has taken place during tensile loading. As mentioned earlier, a strong bonding is established between maleated SEBS elastomers and PA6,6 matrix. These elastomers act as stress concentrators during tensile loading, thereby promoting shear deformation in the matrix. Such a process dissipates a large amount of energy, thus the elongation at break of PA6,6/SEBS-*g*-MA 80/20 blend is considerably higher than that of pure PA6,6.

Figure 6(a) and (b) show the fracture surface morphologies of ternary composites containing 5 and 15 wt % GBs, respectively. Most of the GBs remained intact with the matrix [Fig. 6(a)], although few voids associated with debonding of GBs from the matrix are observed [Fig. 6(b)]. This indicates that there is some interfacial bonding between GBs and the matrix, but the degree of adhesion is reduced when the filler content is increased. It can also be seen from Figure 6(b) that the fracture surface of the matrix of composite is very rough, implying local plastic deformation has taken place in the matrix material around the GBs during the tensile loading process. Therefore, the GB additions do not lead to a

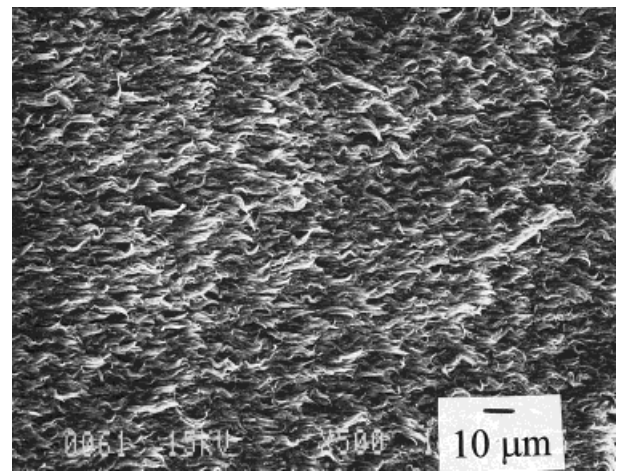
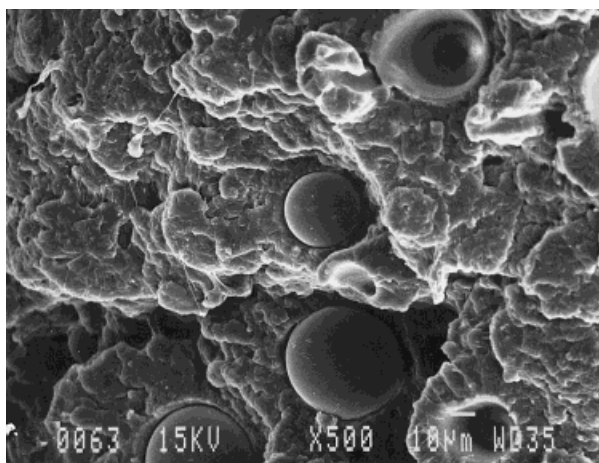
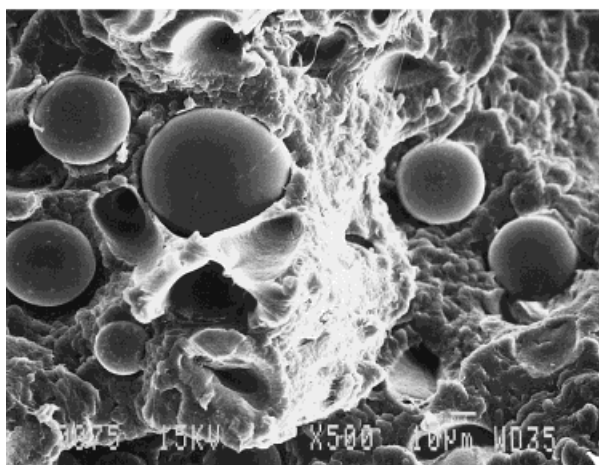


Figure 5 SEM fractograph of PA6,6/SEBS-*g*-MA blend.



(a)



(b)

Figure 6 SEM fractographs of ternary composites filled with (a) 5 wt % GB and (b) 15 wt % GB.

deterioration in the tensile ductility of PA6,6/SEBS-*g*-MA 80/20 blend.

CONCLUSIONS

Tensile and impact measurements were carried out for injection-molded PA6,6, PA6,6/SEBS-*g*-MA 80/20 blend, and its composites. Tensile tests showed that the addition of maleated SEBS to PA6,6 leads to a dramatic increase in its tensile ductility and impact toughness at the expense of stiffness and tensile strength. Moreover, the stiffness of PA6,6/SEBS-*g*-MA 80/20 blend tends to increase with increasing GB content but the tensile ductility remains nearly unchanged with in-

creasing GB concentrations. The impact test reveals that the impact strength of PA6,6/SEBS-*g*-MA 80/20 blend decreases with increasing GB content. Accordingly, the GB additions are beneficial to maintain a stiffness-to-toughness balance of the PA6,6/SEBS-*g*-MA 80/20 blend.

S. A. Xu thanks the Croucher Foundation of Hong Kong for providing a fellowship to work in this research.

REFERENCES

1. Tjong, S. C.; Meng, Y. Z. *Polymer* 1998, 39, 5461.
2. Tjong, S. C.; Jiang, W. *J Appl Polym Sci* 1999, 73, 2247.
3. Tjong, S. C.; Xu, Y.; Meng, Y. Z. *J Appl Polym Sci* 1999, 72, 164.
4. Borggreve, R. J. M.; Gaymans, R. J.; Schuijjer, J.; Inger-Housz, J. F. *Polymer* 1987, 28, 1489.
5. Dijkstra, K.; ter Laak, J.; Gaymans, R. J. *Polymer* 1994, 35, 315.
6. Tjong, S. C.; Ke, Y. C. *Plast Rubber Compos Process Appl* 1996, 25, 319.
7. Oshinski, A. J.; Keskkula, H.; Paul, D. R. *Polymer* 1992, 33, 268.
8. Oshinski, A. J.; Keskkula, H.; Paul, D. R. *Polymer* 1992, 33, 284.
9. Chiang, W. Y.; Yang, W. D.; Pukanszky, B. *Polym Eng Sci* 1992, 32, 641.
10. Jancar, J.; Dibenedetto, A. T. *J Mater Sci* 1995, 30, 2438.
11. Long, Y.; Shanks, R. A. *J Appl Polym Sci* 1996, 61, 1877.
12. Modic, M. J.; Pottick, L. A. *Polym Eng Sci* 1993, 33, 819.
13. Liang, J. Z.; Li, R. K.; Tjong, S. C. *Polym Int* 1999, 48, 1068.
14. Liang, J. Z.; Li, R. K.; Tjong, S. C. *Polym Compos* 1999, 20, 413.
15. Mouzakis, D. E.; Stricker, F.; Mulhaupt, R.; Karger-Kocsis, J. *J Mater Sci* 1998, 33, 2551.
16. Hashemi, S.; Din, K. J.; Low, P. *Polym Eng Sci* 1996, 36, 1807.
17. Carrot, C.; Jaziri, M.; Guillet, J.; May, J. F. *Plast Rubber Compos Process Appl* 1990, 14, 245.
18. Young, R. J.; Beaumont, P. W. R. *J Mater Sci* 1977, 612, 684.
19. Einstein, A. *Ann Phys (Leipzig)* 1905, 17, 549.
20. Guth, E. *J Appl Phys* 1945, 16, 20.
21. Ishai, O.; Cohen, L. *Int J Mech Sci* 1967, 9, 539.
22. Halpin, J. C.; Kardos, J. L. *Polym Eng Sci* 1976, 16, 344.
23. Nicolais, L.; Narkis, M. *Polym Eng Sci* 1971, 11, 194.
24. Lu, S.; Yan, L.; Zhu, X.; Qi, Z. *J Mater Sci* 1992, 27, 4633.